WHITEPAPER

MODEL-BASED DESIGN OF EMI FILTERS FOR POWER ELECTRONICS CONVERTERS WITH CST STUDIO SUITE

Design and modelling of electromagnetic interference (EMI) filters is one of the most important tasks in power electronics, and a power electronic (PE) converter cannot comply with norms without additional filtering. The development of an EMI filter can take long time and requires a multitudes of simulations, prototypes and tests. This whitepaper introduces a modeling method of EMI filters with EM simulation in CST® STUDIO SUITE®. Compared with conventional design methods, the proposed simulation based approach allows to achieve good results with only little prototyping. This whitepaper provides a comprehensive description of the simulation based EMI filter design method. Effectiveness of this design method is confirmed with measurements of built prototypes. Different simplification scenarios are analyzed in order to assess the impact of different non-ideal effects on insertion loss (IL) and to find an optimum between necessary computation time and modeling accuracy.

INTRODUCTION

The number of power electronics devices connected to the power grid has increased significantly during the last years. The three main reasons for a constantly increasing number of applications for power electronics are the required increase in efficiency, renewable power sources and reduction of semiconductor prices. New wide bandgap transistors have been introduced to increase switching frequency of power electronics devices by a factor of ten in the last decade, and switching frequencies for some power electronics converters have already reached 1 MHz. This introduces several potential EMI issues. Firstly, the constantly rising number of power electronics devices and growing switching frequencies can affect total grid robustness and other devices nearby. Secondly, the normal operation of equipment connected close to the interference source can be disturbed. As a result, passive EMI filters have already become a mandatory component for power electronics devices[1].

The normal level of abstraction and simplification, which gives precise simulation results for the majority of applications, is usually not sufficient for designing and modelling EMI filters. The majority of the existing design procedures of EMI filters can be referred to as structured “trial and error” methods. They require a “looped” design and testing procedure. Developed EMI filters have to be tested together with a PE converter until the level of interference emitted by this converter complies with particular norms. Obviously this approach can lead to an unlimited number of iterations and very high development costs. Moreover, every iteration requires prototyping of the previously simulated EMI filter in order to improve the accuracy of the model. In this way, mutual couplings and nonlinear permeability effects are extracted from a built prototype and an equivalent circuit of the filter is fine-tuned in accordance with measurements.

The final tuned model reproduces IL of the EMI filter quite precisely but some minor changes require the whole procedure be restarted. This approach has some clear shortcomings. Firstly, time required for suitable design is almost impossible to predict. Secondly, component requirements mean it is not always possible to build a prototype. Lastly, validation of the electromagnetic compatibility (EMC) concept can be started only when a first converter prototype has been built, which is a problem if the PE converter for the designed filter utilization is unknown or under development. A virtual electromagnetic prototyping of EMI filters based on the finite element method (FEM) has a number of advantages in comparison with conventional EMI filter design procedures. A design flow based on CST STUDIO SUITE enables a comprehensive EMI filter analysis including effects of self-parasitics, frequency-dependent permeability, mutual couplings, PCB layout, etc. Values of passive components can be adjusted using an optimization tool in order to maximize IL of a particular filter without building prototypes. Moreover, IL can be easily assessed not only for the standard 50 Ω load and source impedances but for the worst case scenario. Improvement measures can be straightforwardly implemented and validated using FEM simulation.

CONSIDERATION OF NON-IDEAL PROPERTIES OF AN EMI FILTER

In a frequency range of interest described in the CISPR17:2011 a number of physical effects is relevant for EMI filter performance, such as:

- Saturation effects of a common mode choke (CMC) core
- Frequency degradation of permeability
- Self-parasitics of passive components (equivalent series inductance (ESL) and equivalent series capacitance (EPC))
- Mutual couplings between components within a filter
- Connection to the ground defined by mechanical design

All those parasitics can be considered in CST STUDIO SUITE except maximum saturation flux density B_{max}, which must be assessed analytically as (1). B_{max} consists of two parts: flux induced by common mode current B_{CM} (2) and flux induced by differential mode current B_{DM} (3).

$$B_{\mathrm{max}} = B_{\mathrm{CM}} + B_{\mathrm{DM}}\,, \qquad (1)$$

$$B_{\mathrm{CM}} = \frac{L_{\mathrm{CM}} I_{\mathrm{CM}}}{N A_{\mathrm{e}}} = \frac{\mu_0 \mu_{\mathrm{r}} I_{\mathrm{CM}} N}{l}, \qquad (2)$$

$$B_{\mathrm{DM}} = \frac{L_{\mathrm{DM}} I_{\mathrm{DM}}}{N A_{\mathrm{e}}} = 3\frac{\mu_0 I_{\mathrm{CM}} N}{l_{\mathrm{eff}}}\,, \qquad (3)$$

where L_{CM} and L_{DM} are CM and DM inductance; N is a number of turns per winding; A_e cross section area; μ_0 the permeability constant; μ_r relative permeability; l the main path length of a magnetic core. I_{CM} is the CM current flowing through the CMC and I_{DM} is the differential mode current, which can be approximated by the nominal phase current. l_{eff} can be found according to (4).

$$l_{\mathrm{eff}} = l_{\mathrm{e}} \sqrt{\frac{\theta}{2\,\pi} + \frac{1}{\pi}\sin\frac{\theta}{2}}, \qquad (4)$$

with θ is the angle occupied by a winding. B_{max} must be lower than saturation flux density of the used core material B_{sat}. In order to get high core utilization a margin between B_{max} and B_{sat} should be kept within 30% of B_{sat}

$$B_{\mathrm{sat}} \cdot 0.7 \le B_{\mathrm{max}} < B_{\mathrm{sat}} \qquad (5)$$

Alternatively a number of turns with no saturation can be calculated for a particular choke according to (6)

$$N = \frac{B_{\mathrm{sat}}\, l_{\mathrm{eff}}\, l}{\mu_0 \mu_{\mathrm{r}} (3 I_{\mathrm{DM}} l + I_{\mathrm{CM}} l_{\mathrm{eff}})}\,, \qquad (6)$$

The number of turns N equals to the next integer smaller than obtained in (6) has to be taken. Some approximated value of CM current has to be assumed for analytical EMI filter design. Typically it lies within 5% from a phase nominal current. Alternatively, saturation can be modeled numerically with the low frequency solvers in CST STUDIO SUITE or using hysteresis model of diverse complexity.

Frequency dependency of permeability can be expressed employing the complex permeability μ= μ'+ jμ". Each part of the complex permeability can be represented in terms of the frequency dependent resistor and inductor (7, 8).

$$\mu'(f) = L_{\mathrm{s}}(f)\left(\frac{l}{\mu_0 h_{\mathrm{c}} N^2\, \ln\left({r_{\mathrm{cout}}}/{r_{\mathrm{cin}}}\right)}\right), \qquad (7)$$

$$\mu''(f) = R_{\mathrm{s}}(f)\left(\frac{l}{2\,\pi f \mu_0 h_{\mathrm{c}} N^2\, \ln\left({r_{\mathrm{cout}}}/{r_{\mathrm{cin}}}\right)}\right), \qquad (8)$$

where L_s and R_s are series inductance and resistance, r_{cout}, r_{cin} and h_c are geometrical parameters of a core. Some manufacturers include permeability characteristics in datasheets[2]. Otherwise, resistive and inductive components of the core impedance can be measured. Thereafter real and imaginary parts of permeability can be found from (7), (8).

The theoretical background of equivalent series inductance (ESL) and equivalent series capacitance (EPC) are well described in the literature[3]. Effects of EPC and ESL on IL degradation are rather well investigated[4–6]. ESL and EPC are relatively simple to model and to measure. Self-parasitics depend mainly on geometry. Value of ESL for film capacitors used in EMI filters is typically in the range of 8 – 18 nH. ESL of capacitors in the majority of situations can be found in a datasheet. Alternatively, ESL can be derived from measured resonance frequency according to (9).

$$L_{\mathrm{ESL}} = \frac{1}{(2\,\pi\, f)^2 C} \qquad (9)$$

Measured characteristics of conventional film capacitors with different capacitance values and calculated ESL are depicted in Figure 1. These values are included later into simulation with CST STUDIO SUITE.

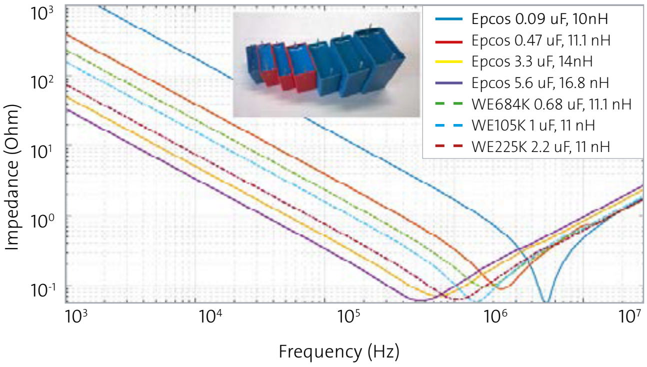

Figure 1: Impedance of capacitors with different ESL and capacitance values.

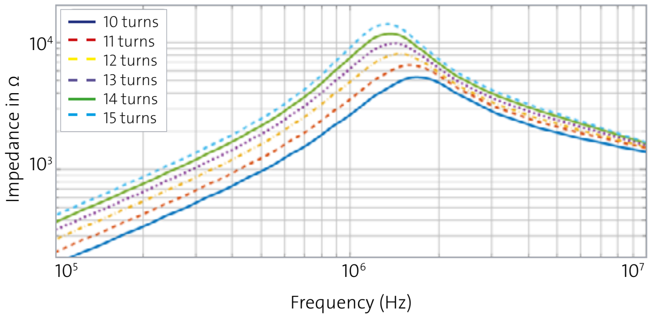

Figure 2: Impedance of a CMC with different turn numbers.

In contrast to capacitors, CMCs are specially designed during filter development. Therefore, the whole CMC design procedure including EPC estimation requires more detailed discussion. EPC has to be estimated for a particular CMC depending on geometry and the number of turns. EPC of a CMC consists of two stray capacitors turn to turn C_{tt} and turn to core C_{tc}. From Figure 2 it can be seen that the number of turns has a minor impact on the self-resonance frequency (SRF) of a CMC. The SRF is shifted due to decrease of inductance but for all studied cased (10…15 turns) EPC is changed insignificantly. These effects are explained by series-parallel connection of C_{tt} and C_{tc} capacitors[7]. Physical parameters necessary for calculation of EPC are shown in Figure 3.

According to[7], turn to turn capacitance consists of the coating capacitance and the capacitance of the air gap between two adjacent turns connected in series and can be estimated with equation (10). According to laboratory measurements, the coating thickness for an actual enamelled copper wire lies in the range from 2% up to 10% of a cable diameter.

$$C_{tt-simpl} = \epsilon_0 l_t \left(\frac{\epsilon_r \theta^*}{\ln \frac{D_o}{D_i}} + \cot\left(\frac{\theta^*}{2}\right) - \cot\left(\frac{\pi}{12}\right) \right), \quad (10)$$

$$\theta^* = \cos^{-1}\left(1 - \frac{\ln \frac{D_o}{D_i}}{\epsilon_r} \right) \quad (11)$$

where θ* is given by (11); ε_0=8.85·10^{-12} As/Vm free space permittivity; ε_r relative permittivity of the coating dielectric; l_t the mean-turn length; D_o and D_i are diameters of a wire with and without insulation respectively.

The stray capacitance between a turn and a core is modeled as a capacitor between a plane and a conductor. Then the path lengths of the electric field lines is only half as in the case of two adjacent turns. Capacity is inversely proportional to the distance between plates and consequently C_{tc} should be double C_{tt}. Overall EPC can be represented by means of equivalent circuits consisting of parallel and series connection of C_{tt} and C_{tc}. For a single-layer winding the value of EPC

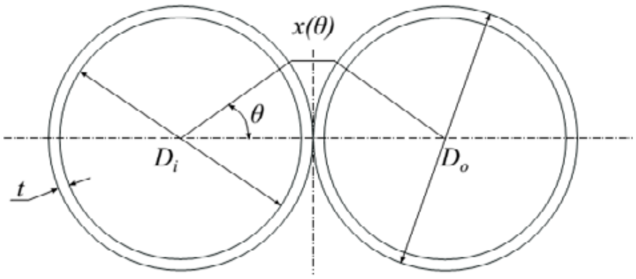

Figure 3: Physical parameters of a CMC for EPC estimation.

is decreasing with increase of a turn number, starting from 2 C_{tt} and stops 1.366 C_{tt} for a number of turns higher than 10.

Physical phenomena behind mutual couplings are well investigated. Mutual couplings depend on arrangement of components within an EMI filter. Moreover, recommendations for component placement in order to diminish such couplings are available[8, 9]. Mutual couplings are automatically considered during FEM simulation.

MODEL PREPARATION

Two three-phase EMI filters are analyzed using the design procedure with CST STUDIO SUITE. The first reference is a self-made PCB-based filter and the second filter is a conventional three-phase EMI filter.

In order to reduce simulation time, the 3D model can be simplified. On the other hand, simplification of a 3D model can lead to inaccurate modelling results. Therefore, a compromise between model accuracy and computation time should be found. An initial 3D model of the EMI filter has to be properly adapted for FEM simulation as follows: Firstly, the majority of non-conductive parts inside of the filter do not influence the electromagnetic fields propagation and can be simplified (except PCBs).

Although losses in dielectric material start to affect IL after several MHz, modelling capacitors as simple rectangles gives good agreement with measurement, and the structure inside of a capacitor can be simplified[10]. The cut in the middle of a rectangle representing a capacitor is used for implementation of a discrete port. A lump capacitor is connected to this port later in the schematic. Utilization of lump components allows the optimization of components values at the final simulation stage and some adjustment of IL.

Lastly, a degree of simplification for CMC windings has to be chosen in order to get adequate EPC. Capacitors simplified to rectangles and CMCs exactly reflecting geometry of real chokes produce quite good results. 3D models used for further modelling are depicted in Figure 4. The number of tetrahedrons after the meshing process is 361,000 for the self-made filter and 530,000 for the conventional filter in order to determine the impact of further geometry simplifications such as windings of CMCs are substituted with rectangular ones or dielectric materials are completely removed etc.

These measures allow the number of cells to be reduced by a factor of 1.8 and the simulation time is reduced by a factor of 2.5, although results are less precise. Figure 5 demonstrates the difference in simulated IL between reference and simplified 3D models. Despite on relatively small mismatch between characteristics obtained from reference and (over) simplified models, some instability of simulation, especially on low frequencies is observed. Therefore, no further simplification of the model depicted in Figure 4 is recommended.

By definition, electromagnetic field energy is transmitted within the EMI filter between its terminals. Ideally this process takes place only between inputs and outputs of a particular phase. In reality, all six terminals of an EMI filter (for a three-phase filter) are coupled. For characterisation of such system, a multiport network can be utilized. There are two types of ports in CST STUDIO SUITE: discrete and waveguide ports. A discrete port represents a lump element connected between two edges of a 3D model. A waveguide port represents an infinitely long waveguide with negligibly small reflection. Use of a waveguide port is recommended for high frequency models (from hundreds of kHz up to GHz range). But the standardized range for conductive EMI pollution does not exceed 30 MHz. Therefore modelling with waveguide ports might be unstable, especially in the kHz range. Moreover, the duration of a simulation with waveguide ports is almost a factor two longer than with discrete ports, so use of discrete ports is recommended. A difference between IL obtained from simulations with waveguide and discrete ports for the same reference filter is shown in Figure 6. Results from a simulation with discrete ports are more stable. Also, there is a mismatch on the low frequency when waveguide ports are utilized. It can be concluded that discrete ports are more suitable for modelling of EMI filters from both accuracy and computation time points of view.

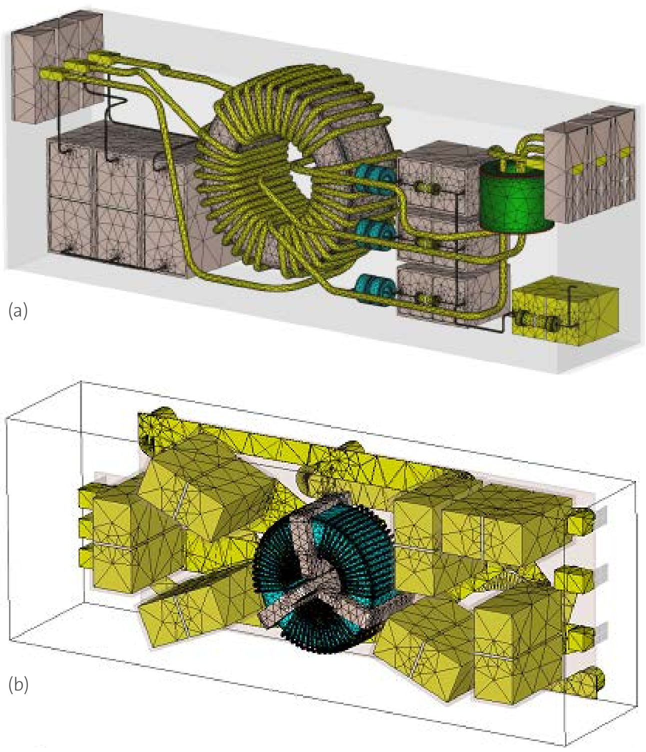

Figure 4: 3D models of EMI filters used for FEM simulation.

(a) 3D Model of EMI filter Schaffmer FN3258

(b) 3D Model of self-made EMI filter

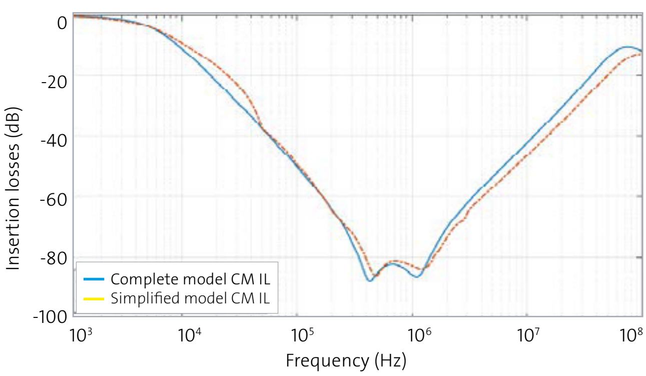

Figure 5: Impact of geometry simplification on common-mode IL.

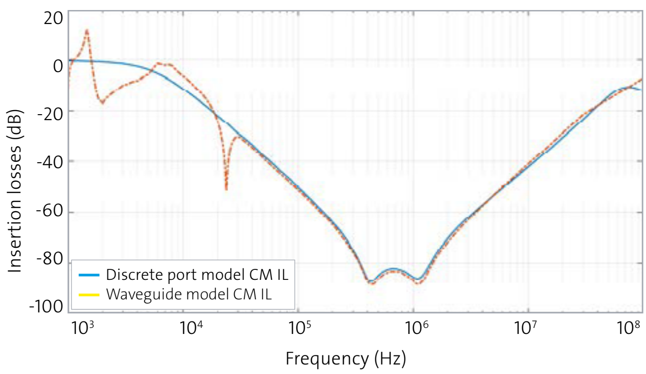

Figure 6: Comparison between common-mode IL simulations with waveguide and discrete ports.

SIMULATION AND POST PROCESSING

For comprehensive understanding of processes in an EMI filter, analysis of IL is conducted in the frequency range from 1 kHz up to 100 MHz, which is wider than the standardized conductive EMI range. This allows better understanding of filter behaviour. A general purpose frequency domain solver with no adaptive meshing is used. Results of the 3D simulation in CST STUDIO SUITE are represented as a frequency dependent matrix consisting of scattering parameters. This matrix can be used for further simulation of both CM and DM IL of a filter in combined simulation. The black-box model obtained from 3D modelling is automatically integrated into schematic, where all necessary lumped components can be included. All model ports previously assigned in 3D are reflected in the black-box model as circuit pins (Figure 7). After normalization of the S-parameter matrix to 50 Ω, DM and CM IL can be calculated based on calculated earlier scattering parameters. When all necessary lumped components are included into schematic, the modelled filter is connected to external port in serial with 50\50 Ω load and source impedances. This circuit reproduces a measurements setup from CISPR 17:2011, as shown in Figure 8. It must be mentioned that a connection of lump components between a port and the ground on schematic is interpreted by software as a lump component connected between two sides of the same port in 3D model.

Frequency depended permeability $\mu(f)$ is typically simplified during the design and simulation process to initial permeability μ_i. In order to evaluate importance of frequency dependent permeability effects, simulations with both idealized and real frequency-dependent permeability are conducted. Initially core permeability is modelled as a constant equal to μ_i. In order to obtain frequency dependent permeability, real and imaginary permeability parts of a real core (EPCOS N87) are measured. This data is used in the magnetic dissipation fit, which uses a model of 6th order for this material. The difference IL simulated for two filters with ideal and frequency dependent permeability models is quite significant (Figure 9).

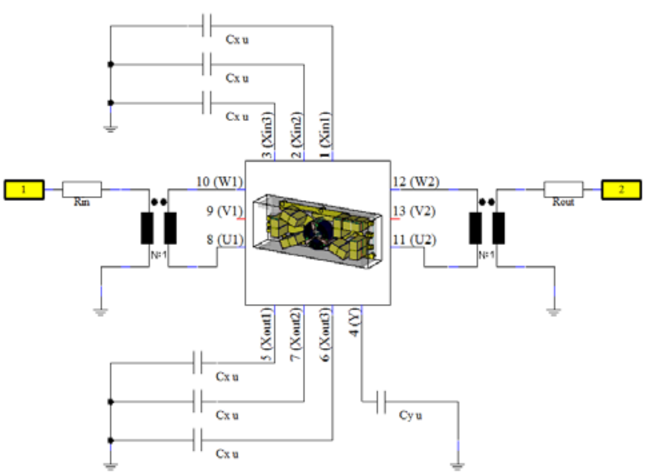

Figure 8: Black-box model of an EMI filter automatically created in schematic.

IL obtained from simulation with idealized permeability is better for both CM and DM. Non-linear permeability leads to lower IL at the range 1 – 100 MHz comparable with the idealized scenario. It can be concluded that utilization of the real permeability characteristics is indispensable for EMI filter design. Simplification at this stage can lead to significant simulation errors.

In order to improve CM IL of the filter, a ferrite core is substituted with a nanocrystalline core. In this case several effects corresponding to theoretical expectations are observed. Firstly, the low frequency CM IL is improved since μ_i of nanocrystalline is much higher. High frequency CM IL remains basically without changes. Secondly, DM IL degrades due to drop of leakage inductance of a CMC. Consequently, nanocrystalline core with higher permeability does not give significant improvement in the high frequency range. In order to improve high frequency IL, a black-box model of a filter can be supplemented with idealized stages and simulated only in schematic. Values of those components are

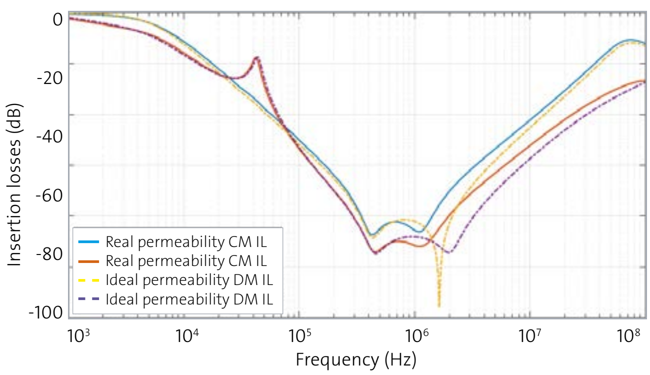

Figure 9: Impact of frequency dependent permeability on common-mode IL.

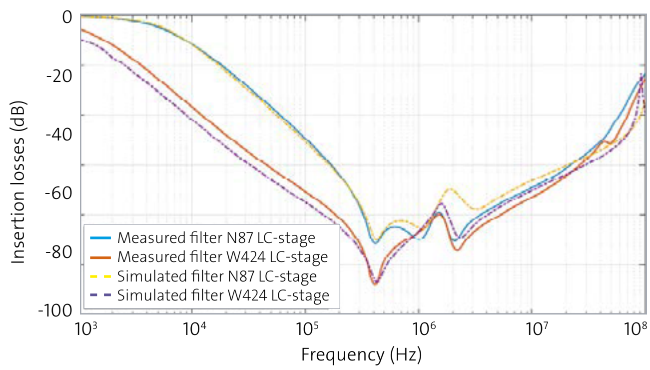

Figure 10: Comparison between common-mode IL of designed and simulated filters with an improvement.

automatically selected by an integrated optimizer, according to boundary conditions given for IL. Minimization of IL in the range 5 – 10 MHz was given as a task. Stray parameters of components used for IL improvement are taken from datasheets and included into schematic for improvement of accuracy. The resulting CM IL for several improved filters are shown in Figure 10. In this way an improvement potential can be estimated before building a new 3D model.

VALIDATION

Resulting measurements for DM and CM IL compared with IL received from simulation are shown in Figures 11 and 12. Both measurements and simulations are conducted according to CISPR 17:2011. Measured characteristics of both self-made and off-the-shelf filters are in good agreement with simulation. Measurements with decoupling networks (unbalanced) do no match with simulation on the low and very high frequencies. It caused by non-ideal decoupling transformers, which are used for measurements. Due to non-ideal effects of transformers only DM IL measured in the linear range of transformers can be used for comparison with simulated IL. The small mismatch by CM and unbalanced DM IL can be explained by a non-ideal measurement setup and by some unaccounted inductance of the ground path.

Two different improvement measures (according to optimization conducted previously) are implemented in the self-made EMI filter. The CM IL improvement predicted in simulation is confirmed by measurements of an improved prototype. The general tendancy is quite similar (Figure 11), with the remaining mismatch caused mainly by the quick, approximate implementation of extra stages (no parasitics are optimized).

The entire workflow of EMI filter design based on CST STUDIO SUITE is summarised in a flow chart, depicted in Figure 13. Characteristics of the simulated filter can be included into a model of a complete power electronics system.

CONCLUSION

The whole workflow of EMI filter design based on CST STUDIO SUITE was shown. The proposed modelling method takes into account all physical effects within a real EMI filter such as nonlinear permeability and intercomponent couplings in the frequency range of 1 kHz – 100 MHz, and allows IL of EMI filters to be simulated with high precision. Good accuracy of modelled IL was confirmed by experimental validation of prototypes. Modelling conditions of the proposed method correspond to requirements, described in CISPR 17:2011. Potential of IL improvement through implementation of additional stages was shown. An optimization tool from CST STUDIO SUITE was used in order to get values of these additional components. Improvement measures implemented in the EMI filter prototype showed performance close to simulation results.

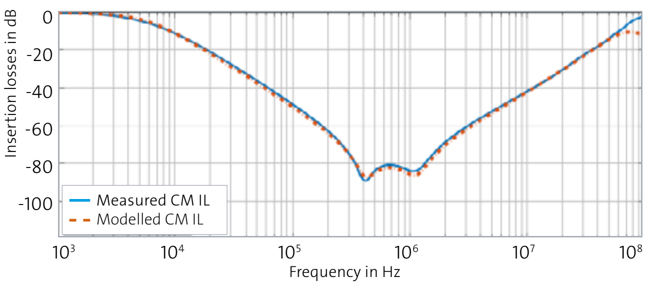

(a) Common mode IL

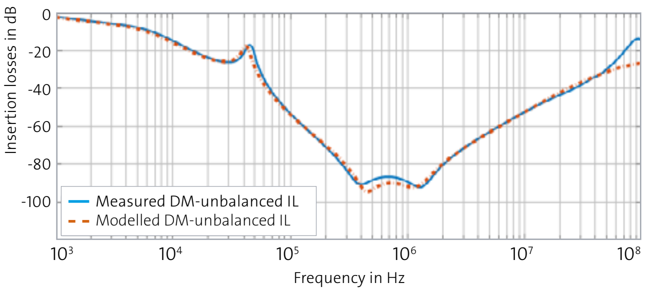

(b) Differential mode IL

Figure 11:

Comparison between designed and simulated IL of the self-made filter.

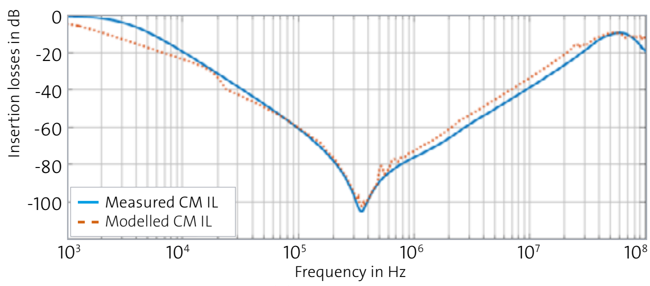

(a) Common mode IL

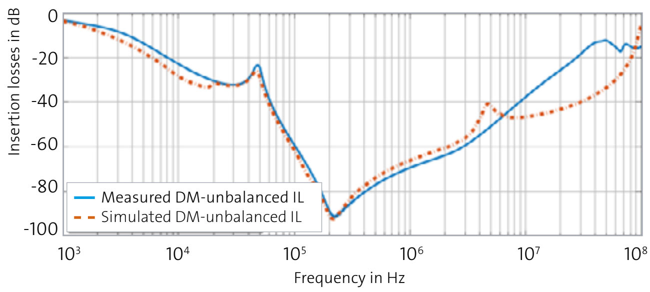

(b) Differential mode IL

Figure 12:

Comparison between designed and simulated IL of the off-the-shelf filter.

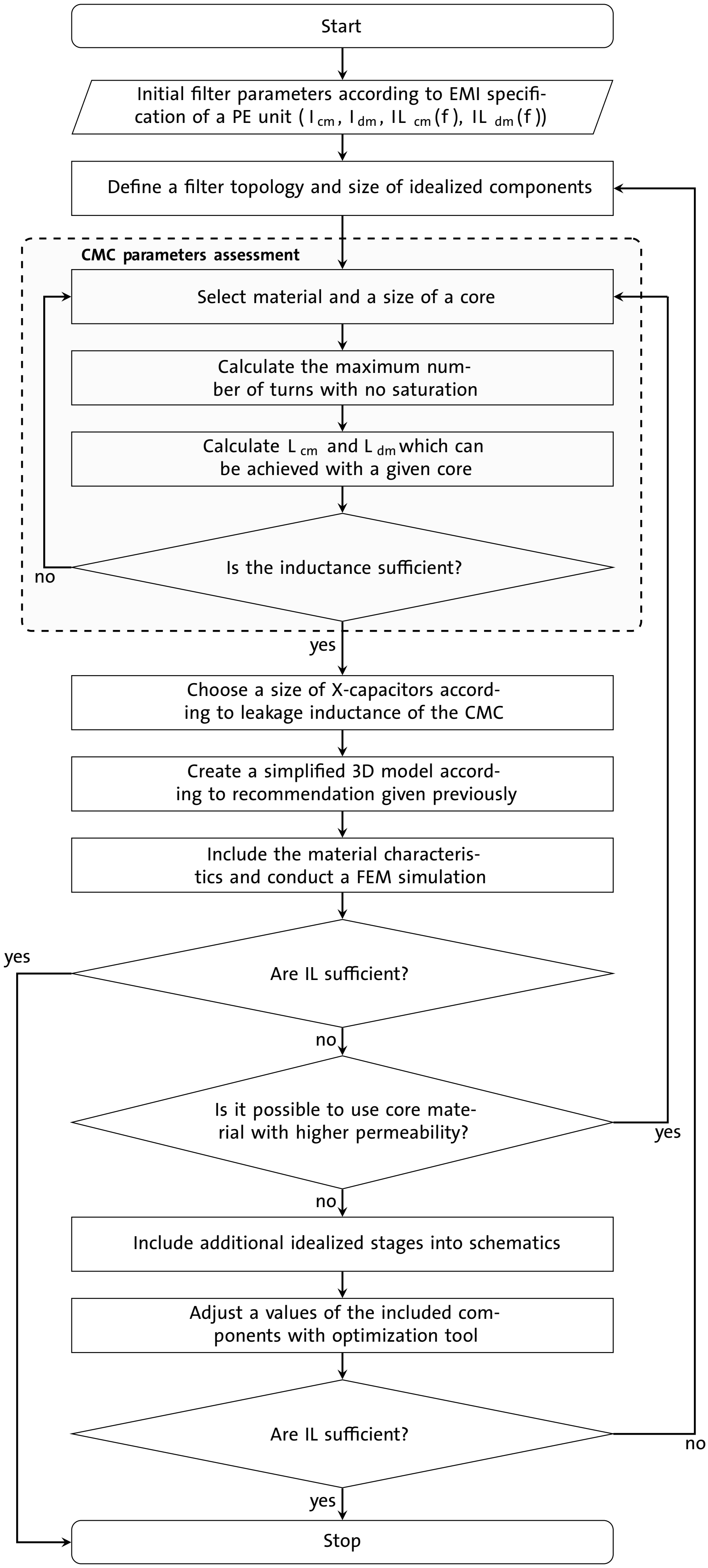

Figure 13: Flow diagram of the entire filter design workflow.

REFERENCES

[1] Information technology equipment – Radio disturbance characteristics – Limits and methods of measurement, CISPR 22:2008, 2008.
[2] EPCOS AG, "Ferrites and accessories: SIFERRIT material N87," 2006.
[3] H. W. Ott, Electromagnetic compatibility engineering. Hoboken, N.J.: John Wiley & Sons, 2009.
[4] T. C. Neugebauer and D. J. Perreault, "Filters With Inductance Cancellation Using Printed Circuit Board Transformers," IEEE Trans. Power Electron., vol. 19, no. 3, pp. 591–602, 2004.
[5] T. C. Neugebauer and D. J. Perreault, "Parasitic capacitance cancellation in filter inductors," IEEE Trans. Power Electron., vol. 21, no. 1, pp. 282–288, 2006.
[6] I. N. Manushyn, L. M. Koleff, G. J. Griepentrog, "Holistic approach to three-phase EMI filter improvement," in PEMD 2016 Glasgow, pp. 1–6.
[7] S. W. Pasko, M. K. Kazimierczuk, and B. Grzesik, "Self-Capacitance of Coupled Toroidal Inductors for EMI Filters," IEEE Trans. Electromagn. Compat., vol. 57, no. 2, pp. 216–223, 2015.
[8] H. Chen, Z. Qian, Z. Zeng, and C. Wolf, "Modeling of Parasitic Inductive Couplings in a Pi-Shaped Common Mode EMI Filter," IEEE Trans. Electromagn. Compat., vol. 50, no. 1, pp. 71–79, 2008.
[9] A. Lissner, E. Hoene, B. Stube, and S. Guttowski, "Predicting the influence of placement of passive components on EMI behaviour," in Power Electronics and Applications, 2007 European Conference on, 2007, pp. 1–10.
[10] G. Asmanis, A. Asmanis, and D. Stepins, "Mutual couplings in three phase T-type EMI filters," in 2012 International Symposium on Electromagnetic Compatibility – EMC EUROPE, pp. 1–6.

AUTHOR

I.N. Manushyn, *Technical University of Darmstadt*